Pol. J. Environ. Stud. Vol. 27, No. 1 (2018), 145-154
DOI: *10.15244/pjoes/73905* ONLINE PUBLICATION DATE: 2017-10-26

Original Research

Study on the Migration Characteristics of Cu^{2+} Ions of Backfill Gangue in Subsided Area

Junmeng Li[1,2], Yanli Huang[1,2,*], Tianqi Song[1,2], Deli Yang[1,2], Guoqiang Kong[1,2]

[1]State Key Laboratory of Coal Resources and Safe Mining, China University of Mining and Technology, Xuzhou, 221116, China
[2]Key Laboratory of Deep Coal Resource Mining, Ministry of Education of China; School of Mines; China University of Mining & Technology, Xuzhou, 221116, China

Received: 23 March 2017
Accepted: 20 May 2017

Abstract

Even though solid backfill mining can address some environmental issues of coal mining (like surface subsidence and gangue storage), on the other hand the long exposure of gangue to rain or other surficial water will also result in the leaching of heavy metal ions, which in turn will pose the threat of potential pollution to groundwater. In response to resolving the above-mentioned problem, this paper simulated the concentration distribution and migration principle of Cu^{2+} in various soils by applying COMSOL Multiphysics software, and the results show that the diffusion distance of Cu^{2+} in different soils are ranked as clay, silty clay, loess, and sandy soil. In addition, the concentration will decrease with the increase of depth and the Darcy velocity contours of Cu^{2+} distribute radially and symmetrically in the transverse direction. The velocity gradient of Darcy velocity in different soils is clay soil > Silty clay soil > loess > sandy soil.

Keywords: dissolved release law, Cu^{2+}, migration law, COMSOL Multiphysics

Introduction

The traditional caving mining method will break in-situ stress and in the process of achieving new stress balance, there will occur Collapse basins and funnel-shaped collapse pits [1-4]. Currently, there are more than 800,000 hectares of land collapsed by coal mining activity in China, and the amount is increasing at a speed of 20,000 hectares per year. Ground subsidence has become one of the major environmental geological disasters in mining areas, which seriously damaged land resources and the ecological environment [5-9]. Since the 1980s, the reclamation of subsidence areas has been a priority job by the state, from spontaneous, decentralized reclamation into an organized and centralized reclamation stage [10-12]. So far, gangue has been adopt as the main solid material to backfill mining voids by many Chinese mining companies, like Lu'an and Jixi as well as Pingdingshan mining areas [13-16]. Backfilling measures not only increase the area of cultivated land, but they improve the ecological environment of the mining area. The reclaimed area can even work as construction lands [17-19].

Chen and Li studied the physical and chemical, mechanical, and engineering properties of gangue by lab experiment and engineering practice, and initially established the feasibility analysis of reclaimed area as construction land, site reclamation, site planning, backfill

*e-mail: huangyanli6567@163.com

elevation, and casing thickness determination, backfill foundation treatment, foundation-bearing capacity detection, and a complete set of reclamation systems [20]. Dong, Yu, and Cheng determined that Cu and Zn contents in the gangue storage area were significantly higher than those with gangue [20-22]. The heavy metal content in the roots of the reclaimed sites was not significantly different from that of the control sites. Cui studied the design scheme of a gangue backfill subsidence area and sand mining pit, including the method of governance, the working procedure of gangue backfill, and the utilization of reclaimed land after reclamation [23]. Cui and Fang focused on coal mining subsidence and residual settlement mechanism, and initially established a macro-to-micro control standard to assess the quality of reclaimed land [24]. Jiang and Liu discussed the technical elements of the reclamation of the dynamic subsidence area from the aspects of determining reclamation elevation, reinforcement of building foundation, anti-deformation building, and structural design [25]. In recent years, there are many studies on the physical and mechanical properties of backfilling material, but research on the migration characteristics and flow field distribution of heavy metal ions in the soil in the subsidence area is not enough. Therefore, this paper used a laboratory test and numerical simulation method to study the migration characteristics of Cu^{2+} in the backfilling body, which is of great significance for perfecting the reclamation theory and guiding engineering practice.

Material and Methods

Experimental Study on Dissolution Law of Cu^{2+} in Gangue

According to the results of experimental and numerical simulation in the past, different kinds of heavy metal ions have similar migration laws in different soils, so we chose to study only the typical heavy metal ions Cu^{2+}, which has the highest risk of pollution. To reveal the dissolution principle of Cu^{2+} in gangue, this paper adopts the concentration of heavy metal ions as the main detection index. The experiment proceed by dipping gangue in distilled water (pH 7) under indoor temperature conditions to study the precipitation mechanism of heavy metal ions, which can be used as a reference for selecting the initial parameters for numerical simulation.

Fig. 1. Plasma emission spectrometer.

Experimental Equipment

The equipment mainly included a crusher, separation screen, pH meter, curing box, and plasma emission spectrometer while the required reagent included 0.01 mol/L hydrochloric acid, 0.01 mol/L NH_4OH, and distilled water. The plasma emission spectrometer is shown in Fig. 1.

Experimental Procedure

The gangue was crushed to smaller than 50 mm (Fig. 2). The samples were produced by mixing three gangues of different particle sizes, namely 0-15 mm, 15-30 mm, and 30-50 mm, and dried at 105ºC for 24 h.

Three 1,000 g single-grade gangue samples were placed in a large-capacity plastic bucket, and three solid-liquid ratios of 1:3, 1:5, and 1:10 samples were made by adding 3,000 ml, 5,000 ml, and 10,000 ml distilled water, respectively. The test solutions were collected every 48 hours and sealed in glass bottles, after which the solution was detected by a plasma emission spectrometer (ICP).

According to the current evaluation criteria of water environment quality in China and the results of the test of gangue composition, the main potential pollution components are iron (Fe), manganese (Mn), copper (Cu), zinc (Zn), lead (Pb), cadmium (Cd), arsenic (As), beryllium (Be), mercury (Hg), calcium (Ca), and sodium (Na). The groundwater quality classification index is listed in Table 1.

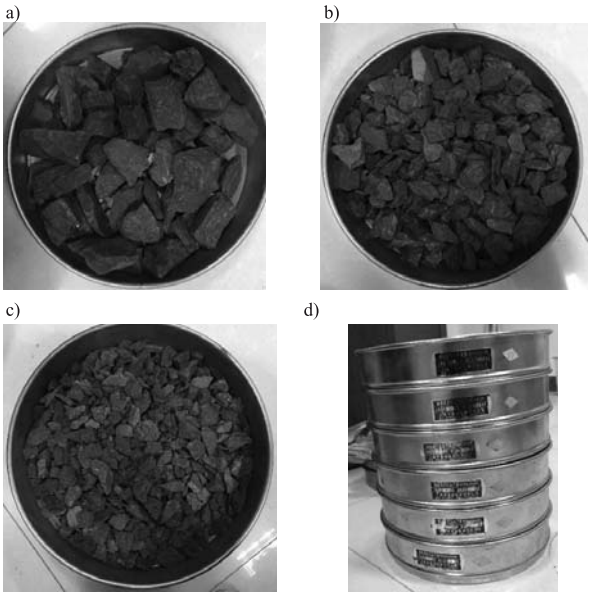

Fig. 2. Preparation of test samples. a) 30~50 mm, b) 15~30 mm, c) 0~15 mm, d) separation screen.

Table 1. Groundwater quality classification index.

Grade	Components	Class I	Class II	Class III	Class IV	Class V
Poisonous	Hg(mg/L)	≤0.00005	≤0.0005	≤0.001	≤0.001	>0.001
	Pb(mg/L)	≤0.005	≤0.01	≤0.05	≤0.1	>0.1
	Cd(mg/L)	≤0.0001	≤0.001	≤0.01	≤0.01	>0.01
	Cr^{6+}(mg/L)	≤0.005	≤0.01	≤0.05	≤0.1	>0.1
	As(mg/L)	≤0.005	≤0.01	≤0.05	≤0.05	>0.05
Poisonous (Excessive amount)	Cu(mg/L)	≤0.01	≤0.05	≤1.0	≤1.5	>1.5
	Zn(mg/L)	≤0.05	≤0.5	≤1.0	≤5.0	>5.0
	Mn(mg/L)	≤0.005	≤0.05	≤0.1	≤1.0	>1.0
	Fe(mg/L)	≤0.1	≤0.2	≤0.3	≤1.5	>1.5
	Se(mg/L)	≤0.001	≤0.001	≤0.01	≤0.1	>0.1
Highly toxic metal	Be(mg/L)	≤0.00002	≤0.0001	≤0.0002	≤0.001	>0.001

Analysis of Results

Under the conditions of static soaking, the dissolution curves of Cu^{2+} in the solid-liquid of each group are shown in Fig. 3, which indicates:

1. The whole dissolution process can be divided into two phases, namely rapid dissolution period (the first eight days) and dissolution equilibrium period (8-12 days). Even though the longer the soaking time the higher the concentration of Cu^{2+}, the release rate will gradually decrease with the increased soaking time. When the particle sizes were 5-20 mm, 20-30 mm, and 30-50 mm, the concentrations of Cu^{2+} were 0.192 mg/L, 0.124 mg/L, and 0.087 mg/L on the eighth day, while on the 12th the concentration would increase to 0.200 mg/L, 0.0.138 mg/L, and 0.141 mg/L, respectively.
2. The concentration of metal ions is negatively correlated with particle size. The smaller the particle size, the larger the specific surface area and the higher the concentration of metal ions. As shown in Fig. 3c), when particle size is 5-20 mm, 20-30 mm, or 30-50 mm, the concentration of Cu^{2+} decreased respectively 0.20 mg/L, 0.141 mg/L, and 0.138 mg/L.
3. When the solid-liquid ratio is different, the release and dissolution law of Cu^{2+} under different particle size conditions remains consistent. However, due to the difficulty in controlling the uniformity of particle size, there are some differences of dissolution law even at the same-level distribution.
4. According to the classification criteria of groundwater quality, the concentration of Cu^{2+} finally stabilized at 0.200 mg/L, 0.138 mg/L, and 0.141 mg/L, which was graded as class III according to the groundwater quality classification.

Numerical Simulation of Cu^{2+} Movement in Soil

On the foundation of laboratory tests, this paper also simulated the movement law of Cu^{2+} in soil by applying COMSOL Multiphysics software. The soil was regarded as a saturated porous medium, and the concentration

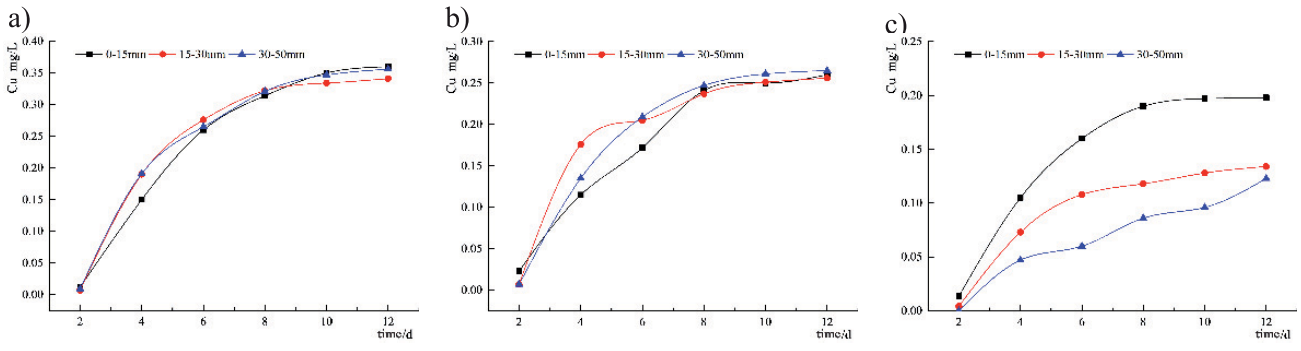

Fig. 3. Dissolution curve of Cu^{2+} in samples with different solid-liquid ratios.
a) solid-liquid ratio = 1:3, b) solid-liquid ratio = 1:5, c) solid-liquid ratio = 1:10.

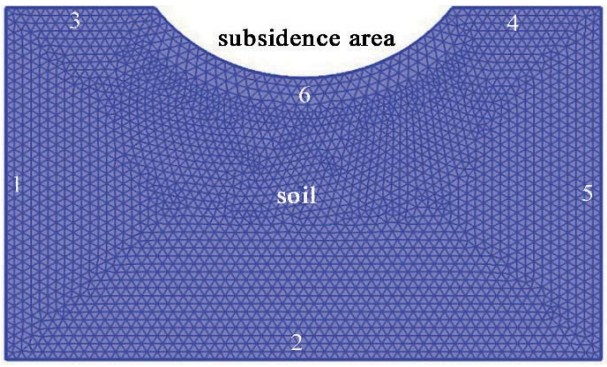

Fig. 4. Geometric model of numerical simulation.

of Cu^{2+} obtained by the dissolution experiment was taken as the initial condition. Considering the negligible influence of the effects of ion species on movement law, Cu^{2+} was chosen as the target object. The team investigated and analyzed the soils of several typical mining areas with collapsed areas, and concluded that most of the soil types at the sites were clay soil, silty clay, loess, and sandy soil. The geometric model, governing equations, calculation parameters, and results of numerical simulation are analyzed as follows:

Geometric Model

According to the actual situation of the subsidence area, the numerical simulation is carried out by using a two-dimensional porous media model with a width of 16 m and depth of 10 m, whereas the radius and depth of subsidence area are 4 m and 2m. The geometric model is subdivided by a free-split triangular mesh. The unit type is a Lagrangian quadratic element, and the grid shape is triangular. The geometric model is composed of 5,654 domain units and 222 boundary elements, which are shown in Fig. 4.

Governing Equations

(1) Equation of Motion

$$\rho(S_e S + \frac{C_m}{\rho g})\frac{\partial p}{\partial t} + \nabla g(\rho u) = Q_m \quad (1)$$

…where ρ is fluid density, S_e is effective saturation, S is the water storage coefficient, C_m is water capacity, g is gravitational acceleration, p is pressure, t is time, u is fluid velocity, and Q_m is seepage flow.

(2) Equation of Continuity

$$\nabla u = 0 \quad (2)$$

The velocity divergence of the continuous equation is 0, which characterizes the conservation of the regional mass during motion.

(3) Controlling Equation for Transferring Chemical Subsidence

$$(\theta + \rho k_{pi})\frac{\partial ci}{\partial t} + (c_i \frac{\partial \theta}{\partial t} - \rho_p k_{pi} \frac{\partial \varepsilon_p}{\partial t}) + \nabla g \Gamma_i + ug\nabla c_i = R_i + S_i \quad (3)$$

…where ρ is fluid density, θ is the volume ratio of the liquid phase, k_{pi} is the isothermal adsorption coefficient of grids, c_i is the concentration of i, ε_p is the porosity of the porous medium, and R_i is the retention factor of the network.

Calculate Parameters

In the simulation of the migration of Cu^{2+} in the soil, the initial conditions of numerical simulation were determined according to the experimental results of the dissolution of heavy metal ions. The backfill material in subsidence area are gangue, which after mechanical crushed and screened with maximum particle size of 15 mm. The gangue in the subsidence area has been in a water environment for a long time. According to the state of backfill in the subsidence area, the soaking results of gangue (solid-liquid ratio of 1:10, particle size of 0-15 mm) were taken as the initial values of the numerical simulation, and the initial concentration was set to 3.125e-6 mol/L. The calculation parameters for different soils were shown in Table 2 [26-27].

Results and Discussion

Analyses on the Results of Numerical Simulation

The migration law of Cu^{2+} in clay, silty clay, loess, and sand was numerically solved by COMSOL Multiphysics, and the concentration distribution of Cu^{2+} in different soils at different times was obtained as shown in Figs 5-8, which show:

1. The concentration of heavy metal ions in the soil decreases with increasing depth along depth direction. Meanwhile, the concentration of heavy metal ions in interface is similar to the initial concentration of heavy metal ions in the subsidence area, and because of the adsorption of soil on metal ions, the concentration will decrease gradually with the increase in depth.

Table 2. Calculation parameters of numerical simulations.

Parameters / Soil type	Density (kg/m^3)	Porosity	Hydraulic conductivity (m/s)
Clay	1,400	34%	1e-8
Silty clay	1,400	42%	6e-7
Loess	1,450	45%	1.25e-6
Sand	1,600	58%	5.26e-6

2. At the end of the simulation, the longitudinal diffusion distances of heavy metal ions in clay soil, silty clay soil, loess soil, and sand soil were 0.69 m, 1.90 m, 3.04 m, and 7.68 m, while the transverse diffusion distances were 0.65 m, 1.63 m, 2.17 m, and 3.41 m, respectively. This is due to the different inhibition effects of various soil permeability coefficients on the movement of heavy metal ions; the greater permeability coefficient of soil, the less suppression there would be, and the longer diffusion distance the heavy metal ions would experience.
3. The longitudinal diffusion distance of heavy metal ions is obviously larger than that of transverse diffusion, and the longitudinal diffusion distance in clay, silty clay, loess, and sand exceed 6.1%, 16.6%, 40.0%, and 125.2% of the horizontal diffusion distance, respectively. This phenomenon can mainly be ascribed to the influence of gravity on the diffusion function:

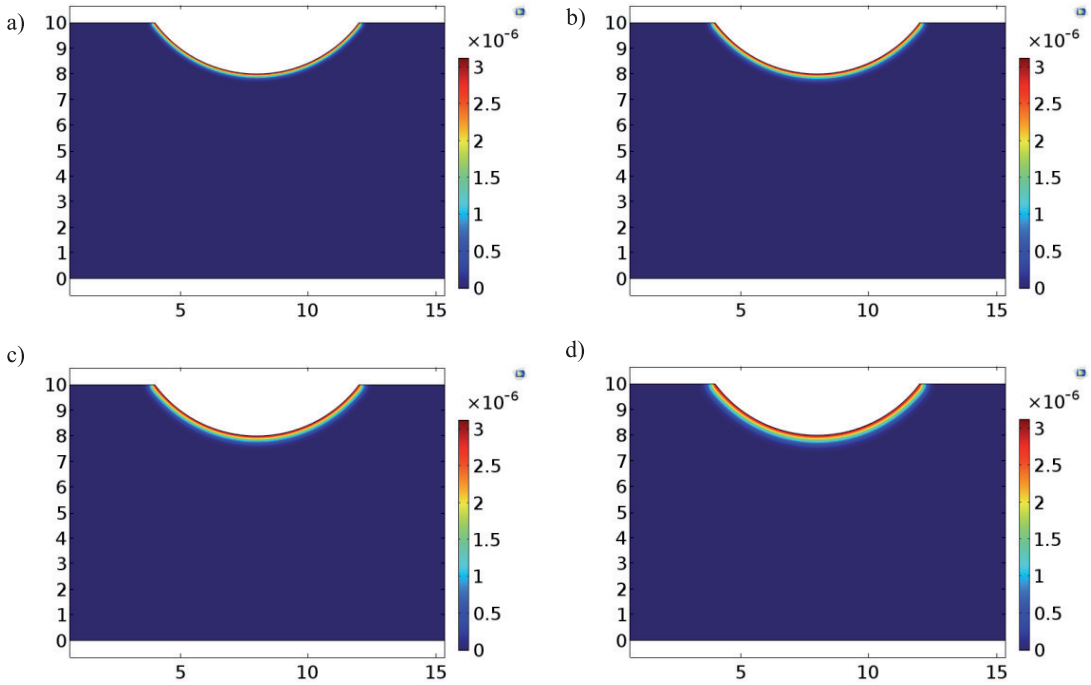

Fig. 5. Concentration distribution of Cu^{2+} in clay. a) 100d, b) 200d, c) 300d, d) 500d.

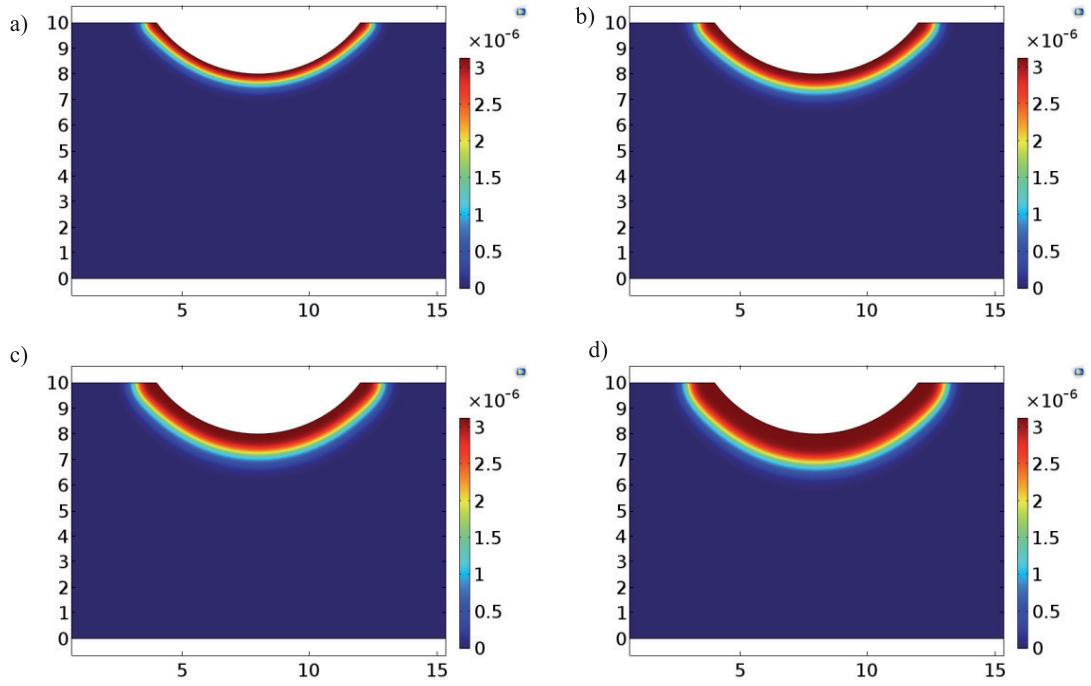

Fig. 6. Concentration distribution of Cu^{2+} in silty clay. a) 100d, b) 200d, c) 300d, d) 500d.

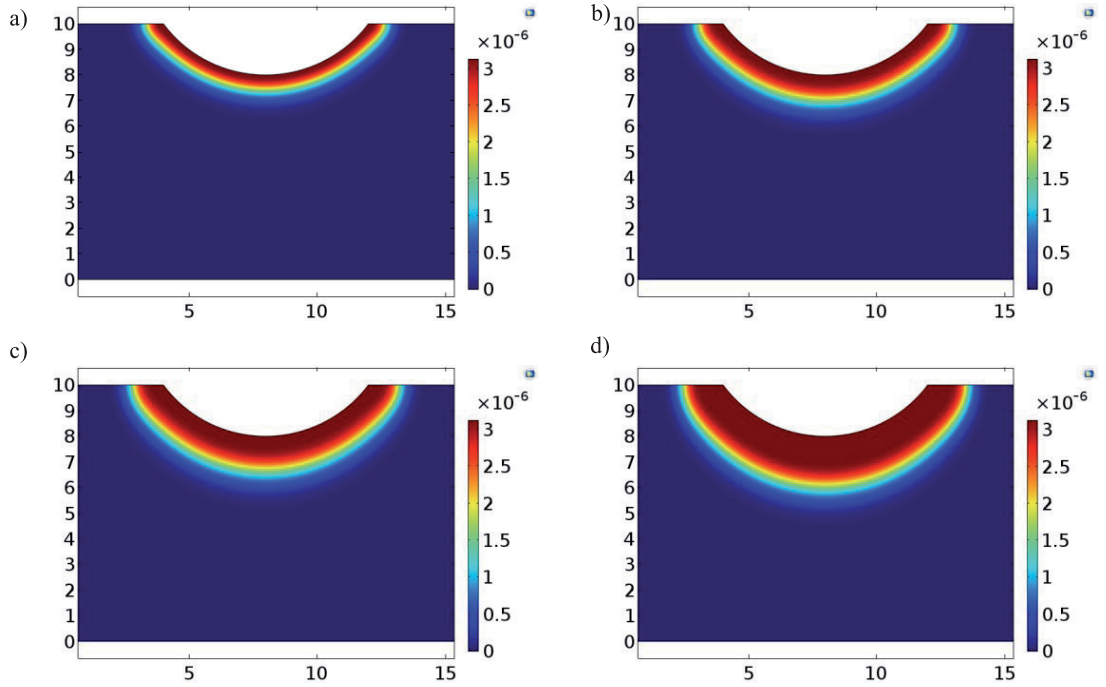

Fig. 7. Concentration distribution of Cu2+ in loess. a) 100d, b) 200d, c) 300d, d) 500d.

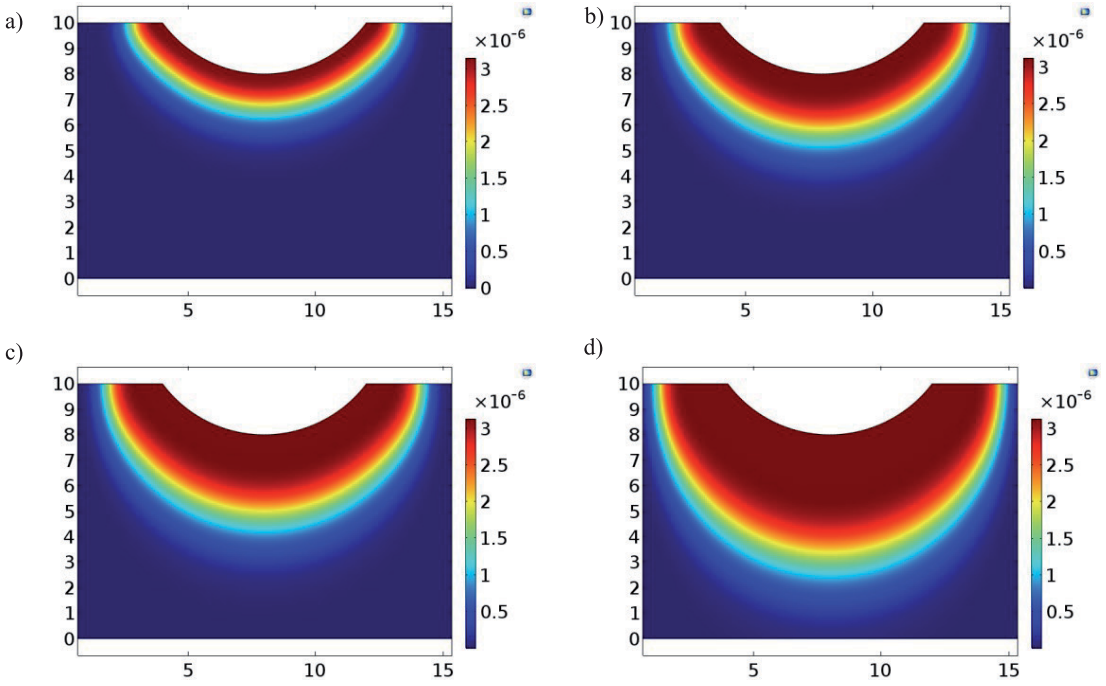

Fig. 8. Concentration distribution of Cu^{2+} in sand. a) 100d, b) 200d, c) 300d, d) 500d.

the general longitudinal diffusion velocity is greater than the transverse diffusion velocity, and the greater the porosity of the soil, the greater the influence would be.

The concentration of Cu^{2+} on the line of y = 7.5 in different soils were shown in Fig. 9, which illustrates:

1. The concentration of Cu^{2+} is symmetrically distributed in the transverse direction, which peaks at the symmetry axis and decreases gradually at both sides. This is due to seepage rate, which is the largest at the symmetry axis and which results in a higher concentration of Cu^{2+}.
2. The influential range of Cu^{2+} is clay < silty clay < loess < sand, and the transverse gradient concentration is clay > silty clay > loess > sand. This is due to the smaller permeability coefficient of soil imposing a greater inhibition on the diffusion movement of heavy metal ions, resulting in the smaller transverse

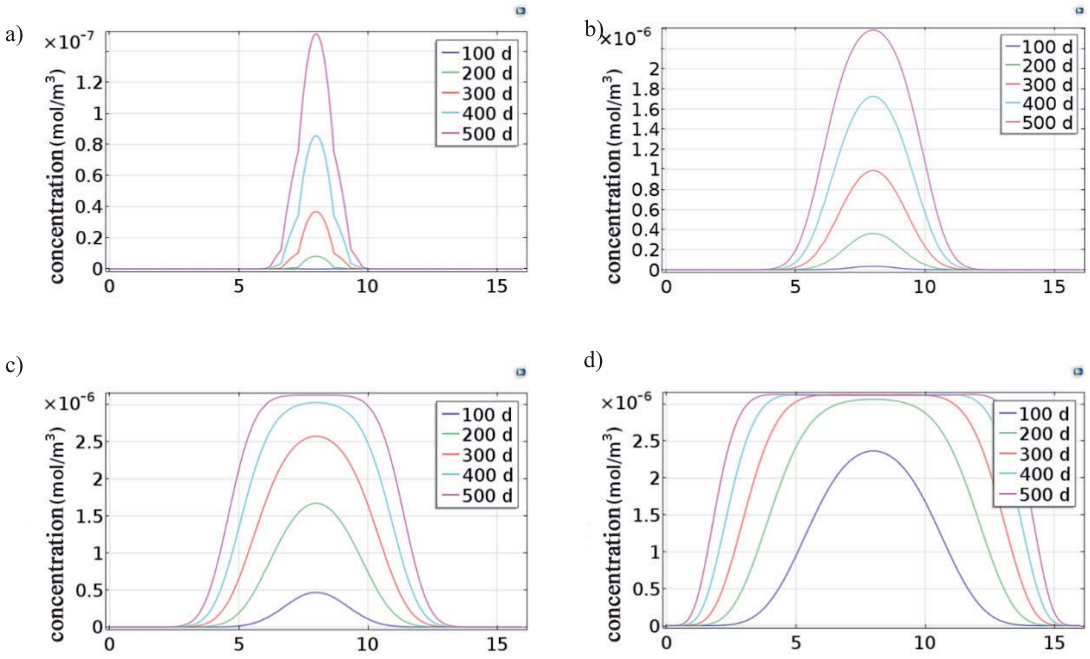

Fig. 9. Concentration profile of Cu^{2+} of the test line at different soils. a) Clay, b) Silty clay, c) Loess, d) Sand.

range of heavy metal ions. While in the condition that the concentration difference is constant, the smaller the influential range, the larger the gradient of concentration.

The migration of Cu^{2+} in clay, silty clay, loess and sand was numerically solved by COMSOL Multiphysics and the contours of seepage velocity of Cu^{2+} in different soils were obtained in Figs 10-13, which show:

1. The Darcy velocity contours in the soil are radially distributed and decrease with the increase of the distance to the subsidence area. This is due to the increase of the distance to the subsidence area, which will reduce the pressure in the soil, resulting in the continuous reduction of Darcy seepage velocity along the direction of depth.
2. The Darcy velocity contours in the soil are symmetrically distributed in the transverse direction, and the velocity peaks at the symmetry axis. This is because the symmetry axis located close to the subsidence area indicates the highest migration speed of Cu^{2+}.
3. The gradient of Darcy velocity in different soils is clay > silty clay > loess > sand. This is due to the smaller permeability coefficient of soil leading to the higher suppression of soil on the diffusion of heavy metal ions.

The Darcy velocity of Cu^{2+} on the line of y = 7.5 in different soils were shown in Fig. 14, which indicates:

1. The Darcy velocity of Cu^{2+} is symmetrically distributed in the transverse direction, the Darcy velocity peaks at the symmetry axis and decreases gradually at both sides. This is caused by the ellipsoid shape of the subsidence area. At the deepest center of the subsidence area, the pressure head is also the largest. According to Darcy's law, it is known that the Darcy velocity increases with the increase of the pressure head, so the Darcy velocity remains highest at the symmetry axis.
2. The Darcy velocity of Cu^{2+} was clay < silty clay < loess < sand, and the corresponding peak values were 5.23×10^{-10} m/s, 9.88×10^{-9} m/s, $1.88\text{x}10^{-8}$ m/s, and $6.21\text{x}10^{-8}$ m/s.

The Darcy velocity of Cu^{2+} at the A point in different soils was shown in Fig. 15, which makes it obvious that:

1. Darcy velocity in the soil increases with time to the maximum and then decreases gradually, which experiences rapid growth stage, decreasing stage, and stabilizing stage. This is due to the large difference in the concentrations of heavy metal ions between the soil and the subsidence area in the initial stage, and the difference would narrow with the passage of time. Therefore, the change in Darcy velocity increases first and then decreases and finally remains steady.
2. At the phase of rapid growth stage, the seepage velocity increases from zero to maximum sharply, and the duration is clay > silty clay > loess > sand. When the concentration difference is constant, the soil with large permeability coefficient is sensitive to the change of Darcy velocity, and can change rapidly according to the change of pressure head, so it can reach the maximum value of Darcy speed in a short time.
3. At the end of numerical simulation, the Darcy velocity of point A in the clay, silty clay, loess, and sand is 5.23×10^{-10} m/s, 9.88×10^{-9} m/s, $1.88\text{x}10^{-8}$ m/s, and 6.21×10^{-8} m/s, respectively. This is because the greater the permeability coefficient of soil, the less suppression of soil on the diffusion of Cu^{2+}, accordingly, and the higher the speed of Darcy.

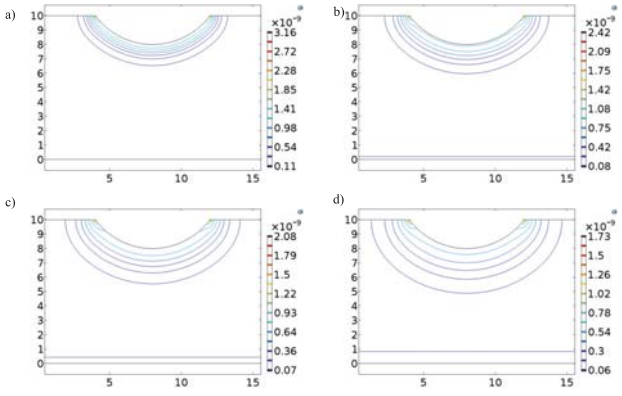

Fig. 10. Contours of seepage velocity of Cu^{2+} in clay. a) 100d, b) 200d, c) 300d, (d) 500d.

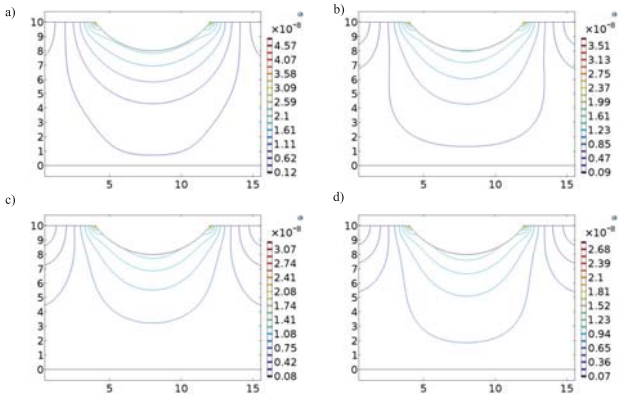

Fig. 11. Contours of seepage velocity of Cu^{2+} in silty clay. a) 100d, b) 200d, c) 300d, d) 500d

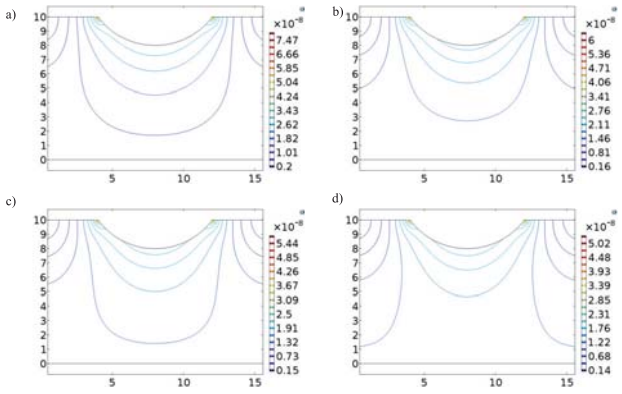

Fig. 12. Contours of seepage velocity of Cu^{2+} in loess. a) 100d, b) 200d, c) 300d, d) 500d.

Conclusions

1. The diffusion distance of heavy metal ions in soils is clay < silty clay < loess < sand, and the concentration decrease with the increase of depth along the depth. At the end of the simulation, the longitudinal diffusion distances of heavy metal ions in clay, silty clay, loess, and sand were 0.69 m, 1.90 m, 3.04 m, and 7.68 m, respectively, while the transverse diffusion distances were 0.65 m, 1.63 m, 2.17 m, and 3.41 m. The longitudinal diffusion distance of heavy metal ions is obviously larger than that of transverse diffusion distance. The longitudinal diffusion distance in clay, silty clay, loess, and sand exceeded 6.1%, 16.6%, 40.0%, and 125.2% of the horizontal diffusion

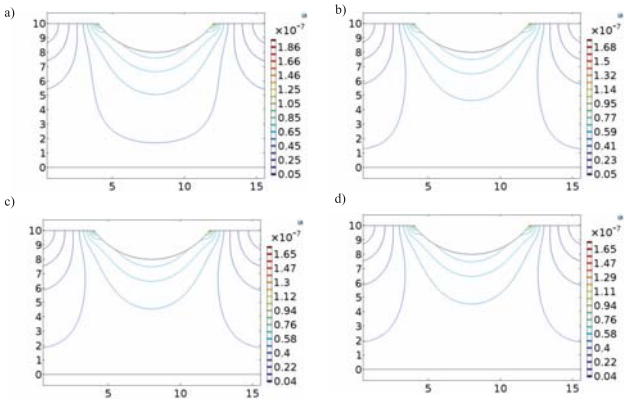

Fig. 13. Contours of seepage velocity of Cu^{2+} in sand. a) 100d, b) 200d, c) 300d, d) 500d.

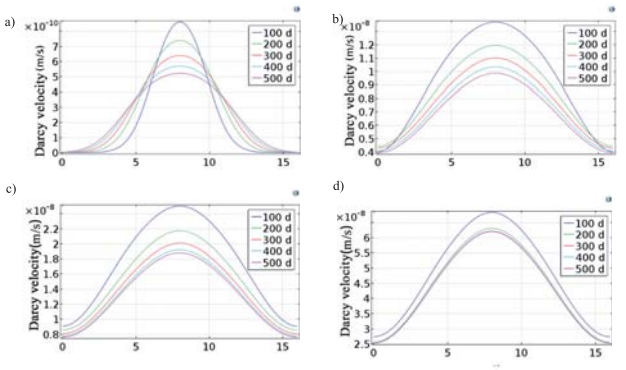

Fig. 14. Darcy velocity of Cu^{2+} in different soils. a) Clay, b) Silty Clay, c) Loess, d) Sand.

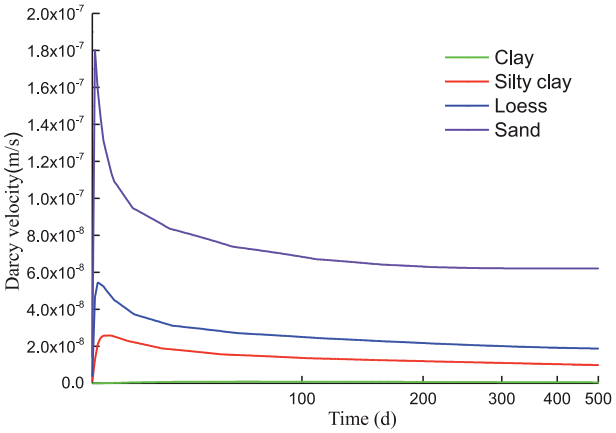

Fig. 15. Darcy velocity of Cu^{2+} at point A in different soils.

distance. In engineering practice, the migration distance of heavy metal ions in different soils can predict whether the aquifer may be polluted according to the soil type of the subsidence area and the distance between the aquifer and the bottom of the subsidence area.

2. The concentration of Cu^{2+} is symmetrically distributed in the transverse direction, which peaks at the symmetry axis and decreases gradually at both sides. The horizontal influential range is clay < silty clay < loess < sand, while the lateral gradient is clay > silty clay > loess > sand. In other words, under the condition that the concentration difference is constant, the smaller the influence range, the larger the gradient of concentration.
3. The contours of Darcy velocity in the soil are distributed radially and are symmetrically distributed in the transverse direction. Meanwhile, the Darcy velocity decreases with the increase of the distance to the subsidence area and it peaks at the symmetry axis and decreases gradually at both sides. The gradient of Darcy velocity in different soils is clay > silty clay > loess > sand.
4. The Darcy velocity in the soil usually increases with time, decreases gradually, and finally remains steady. It includes three phases, namely rapid growth stage, decreasing stage, and stabilizing stage. After the numerical simulation, the velocity values of point A in the soil of clay, silty clay, loess, and sand are 5.23×10^{-10} m/s, 9.88×10^{-9} m/s, $1.88\text{x}10^{-8}$ m/s, and $6.21\text{x}10^{-8}$ m/s.

Acknowledgements

We gratefully acknowledge the financial support for this work provided by the Fundamental Research Funds for the Central Universities (2015XKMS001), the National Natural Science Foundation of China (No. 51774269) and the Qing Lan Project of JiangSu Province.

References

1. GUO Q.B., GUO G.L., LI X. Strata movement and surface subsidence prediction model of dense solid backfilling mining. Environmental Earth Sciences, **75** (21), 1426, **2016**.
2. CHEN B.Q., DENG K.Z., FAN H.D. Combining D-InSAR and SVR for monitoring and prediction of mining subsidence [J]. Journal of China University of Mining & Technology, **43** (05), 880, **2014**.
3. ISHWAR S.G., KUMAR DHEERAJ. Application of DInSAR in mine surface subsidence monitoring and prediction [J]. Current Science, **23** (01), 46, **2017**.
4. STROZIK G., JENDRUS R., MANOWSKA A. Mine Subsidence as a Post-Mining Effect in the Upper Silesia Coal Basin [J]. Polish Journal of Environmental Studies, **25** (02), 777, **2016**.
5. HUANG S.P. Comprehensive management of collapse area should pay attention to the reconstruction of two systems [J]. Ecological Economy, (01), 288, **2010**.
6. LI G.P., LIU Z.G. The loss of ecological environment in the exploitation of coal resources in Northern Shaanxi[J]. Journal of Henan University of science & Technology (Social Science), **24** (04), 74, **2006**.
7. DAI X. Coal mining area ecological recovery and countermeasures research [D]. Harbin Institute of Technology, **2006**.
8. SUN J.C. Ground Sediment Transport Model and Numerical Simulation [J]. Polish Journal of Environmental Studies, **25** (04), 1691, **2016**.
9. JAMROZIK A., ZIAJA J., GONET A. Analysis of Applicability of Modified Drilling Waste for Filling out Annular Space in Horizontal Directional Drilling [J]. Polish Journal of Environmental Studies, **20** (03), 671, **2011**.
10. LIU X., FU J.C., NIU H.P. Analysis on changes of land use structure and assessment of landscape comprehensive stability in Yangquan 1st Mine [J]. Journal of China Coal Society, **41** (03), 719, **2016**.
11. CUI W.J., HUANG J.J., HAN T. The mine environmental geological problems and countermeasures of prevention and control in Xuzhou City [J]. The Chinese Journal of Geological Hazard And Control, **18** (04), 93, **2007**.
12. HU Z.Q. The basic principle and the method of coal mine reclamation soil profile reconstruction [J]. Journal of China Coal Society, 06, 59, **1997**.
13. LIU G.S., LI L., YANG X.C., GUO L.J. Numerical Analysis of Stress Distribution in Backfilled Stopes Considering Interfaces between the Backfill and Rock Walls [J]. International Journal of Geomechanics, **17** (02), 1943, **2017**.
14. DENG D.Q., LIU L, YAO Z.L., SONG K.L., LAO D.Z. A practice of ultra-fine tailings disposal as filling material in a gold mine [J]. Journal of Environmental Management, **196**, 100, **2017**.
15. HUANG Y.L., LI J.M., SONG T.Q., KONG G.Q., LI M. The mine environmental geological problems and countermeasures of prevention and control in Xuzhou City [J]. Energies, **10** (01), 93, **2017**.
16. LI M., ZHANG J.X., HUANG P., GAO R. Mass ratio design based on compaction properties of backfill materials [J]. Journal of Central South University, **23** (10), 2669, **2016**.
17. MA Y.C., ZHANG Y.D., MA Y.K. Research on deformation of foundation in subsidence coal mining area under ground load [J]. China Mining Magazine, **22** (09), 107, **2013**.
18. YAN Y.T., LU J.H., CHEN D.C. Study on land reclamation and ecological reconstruction in Tangshan coal mining subsidence area [J]. Resources·industry, 07, 14, **2000**.
19. ZHOU W., YANG K., BAI Z.K., CHENG H.X., LIU F. The development of topsoil properties under different reclaimed land uses in the Pingshuo opencast coalmine of Loess Plateau of China [J]. Ecological Engineering, **100**, 237, **2017**.
20. CHEN L.S., LI X.L. Techniques of Gangue Backfilling and Reclamation in Subsidence Region of Coal Mined [J]. Metal Mine, **32** (09), 137, **2014**.
21. DONG Q.H., YU M., CHENG W. Safety of heavy metals pollution for wheat planted in reclaimed mining soil [J]. Transactions of The Chinese Society of Agricultural Engineering, **26** (12), 280, **2010**.
22. DONG Q.H., BIAN Z.F., WANG H.F. Comparison of Heavy Metal Contents Between Different Reclaimed Soils and the Control Soil [J]. Journal Of China University of Mining & Technology, **36** (04), 531, **2007**.
23. CUI D. Discussion on the Gangue Utilization in Recovery and Control of Land Subsidence in the Xinwen Mining Area [J]. Journal of Shandong University of Science And Technology(Natural Science), **27** (06), 29, **2008**.

24. CUI L.Z., FANG X. Preliminary Research on Quality Control Standard of the Reclamation Construction Land in Coal Mining Subsidence Area [J]. West anhui university journal, **32** (02), 108, **2016**.
25. JIANG S., LIU L.Z. Techniques of Gangue Backfilling and Reclamation in Subsidence Region of Coal Mined [J]. Journal of China Coal Society, 12, 1622, **2009**.
26. WANG K., ZHANG R.D., WANG F.Q. Continuum fractal model for unsaturated soil hydraulic conductivity [J]. Advances in Water Science, **15** (02), 206, **2004**.
27. FELDGUN V.R., YANKELEVSKY D.Z., KARINSKI Y.S. A new simplified analytical model for soil penetration analysis of rigid projectiles using the Riemann problem solution [J]. International Journal of Impact Engineering, **101**, 49, **2017**.